ORIGINAL ARTICLE

The quantitative evaluation of the cutting surface quality levels in abrasive water jet cutting by measurement of the representative striation mark displacement

Martin Brandstätter[1] · Andreas Wöhrle[1] · Michael Kaufeld[2,4] · Frank Pude[3,4] · Akash Nag[5] · Sergej Hloch[6]

Abstract
Non-thermally affected surfaces created by abrasive water jet, among many other advantages, are manufactured with geometric inaccuracies. These geometric inaccuracies are mainly related to waviness, especially in the lower parts of thick engineering components. Therefore, the study establishes a link between the surface quality and abrasive water jet material disintegration parameters related to striation mark displacement. The materials used for the experiments (aluminum, steel, and polyethylene plastic) are selected to cover a wide range of hardness values. These materials are often machined, which enables to draw practical reference values from the results obtained. Experiments are used for determination of the surface quality to assign a range of surface roughness profile parameters R_z and R_a, as soon as no clear striation marks are recordable on the surface for particular materials with specific mechanical properties.

Keywords Abrasive water jet · Surface quality · Striation mark displacement · Surface roughness · Surface waviness · Design of experiment

Abbreviations

$\dot{m}_a$	Abrasive flow rate (g/s)
u	Angle defect (-)
R_a	Average roughness value (µm)
h_c	Critical depth (mm)
v_c	Cutting speed (mm/s)
t	Cutting thickness (mm)
λ_c	Cutoff wavelength (mm)
h	Depth of cut (mm)
ρ	Density (kg/m^3)
r_k	Edge radius (mm)
h_f	Fine cut length (mm)
d_f	Focusing tube inner diameter (mm)
f	Groove width (mm)
s_b	Jet influenced zone (mm)
λ_s	Lower wavelength filter (µm)
N_m	Machinability (-)
N_m	Machinability number (-)
R_z	Maximum roughness (µm)
W_z	Maximum waviness (µm)
RSm	Mean width of roughness profile (mm)
d	Nozzle diameter (mm)
p_w	Pressure (MPa)
Q	Quality level (-)
g	Ridge (mm)
h_r	Remaining length (mm)
R_b	Rockwell hardness (HRBW)
z	Standoff distance (mm)
n	Striation mark displacement (mm)
l_r	Single measuring distance (mm)
l_n	Total measuring distance (mm)
s	Water side entry (-)
$\dot{m}_w$	Water flow rate (l/min)
v_w	Waterjet velocity (mm/s)
AWJ	Abrasive water jet
DoE	Design of experiment

✉ Sergej Hloch
sergej.hloch@tuke.sk

1 Faculty of Mechanical Engineering and Vehicle Engineering, Ulm University of Applied Sciences, Ulm, Germany

2 Faculty of Mechatronics and Medical Engineering, Ulm University of Applied Sciences, Ulm, Germany

3 Inspire AG, ETH Zurich, Zurich, Switzerland

4 Steinbeis Consulting Center High-Pressure Waterjet Technology, Horgau, Germany

5 Indian Institute of Technology, Dhanbad, India

6 Faculty of Manufacturing Technologies, TUKE With a Seat in Prešov, Prešov, Slovakia

1 Introduction

One of the few tools with the specific properties necessary for engineering material development is the abrasive water jet (AWJ) [1]. AWJ is considered one of the most advanced unconventional manufacturing technological procedures [2]. In recent years, this technology has become an increasingly competitive tool due to its suitability in diverse applications [3–7]; that is, owing to its ability to manufacture component parts out of hard-to-machine materials in any direction, and to the absence of a heat-affected zone or heat deformation with minimum environmental impact [8, 9]. With the parallel improvement of the pumps [10], waterjet cutting has become one of the most powerful cutting methods ever used, with an industrial standard water pressure of $p = 600$ MPa and a cutting capacity of up to 300-mm thickness for softer materials [11]. Nevertheless, this process has remained a rather rare phenomenon for special applications compared to conventional machining and manufacturing [12]. The limitation of a high-speed AWJ is unevenness in the form of striations and roughness [13] generated during the material disintegration caused by many factors [9, 14]. The causes of surface defects limit a broader utilization of the technology of high-speed AWJs in industry [15]. For this reason, and because of the fundamental diversity of editable materials, there is no universal model for AWJ cutting [16]. The most common description of the surface is based on the five quality (Q) levels [17]. There are no clear definitions that relate these Q levels to surface quality and striation mark displacement. In terms of practical applications, the worker should be able to produce a (clearly) required surface and verify it with simple means. The idea

is to determine the most easily measurable surface characteristic, the striation mark displacement, and then be able to draw conclusions about the roughness, waviness, and Q level from it [18]. Hashish first explained the processes and interactions between the abrasive particles and the material in [19], followed by many other authors [20–24]. Kulekci [20] studied the influence of water pressure, grain size, and traverse speed on surface roughness and depth of cut. Hlavac [21] developed theoretical model to calculate the tilt angle of the cutting head enabling the jet to follow trajectory approximately normal to the material surface during its exit after material cutting. Hreha et al. [22] investigated the vibration frequency emission during impact of abrasive particle with the material [25]. It was concluded that the monitoring of the vibration signals can be used as feedback mechanism for online process control. Lemma et al. [23] studied the interlink between the two-phase cyclic material removal mechanism and striation formation. Perec et al. [24, 26] also studied the influence of basic cutting parameters such as traverse speed, abrasive type, and mass flow rate of abrasive on cutting depth while cutting titanium samples. In order to illustrate and better understand the processes of AWJ cutting, the author in [19] carried out cutting experiments with acrylic glass and filmed them. Calculations were based on the energy of the abrasive particles. More specifically, the forces and moments of a particle were determined, and the volume removal was determined by means of the resistance forces. From this preliminary work and some other considerations, the author developed a model by which the cutting depth can be determined. In summary, the following findings can be mentioned. The illustration (Fig. 1) of the cutting process in the acrylic glass
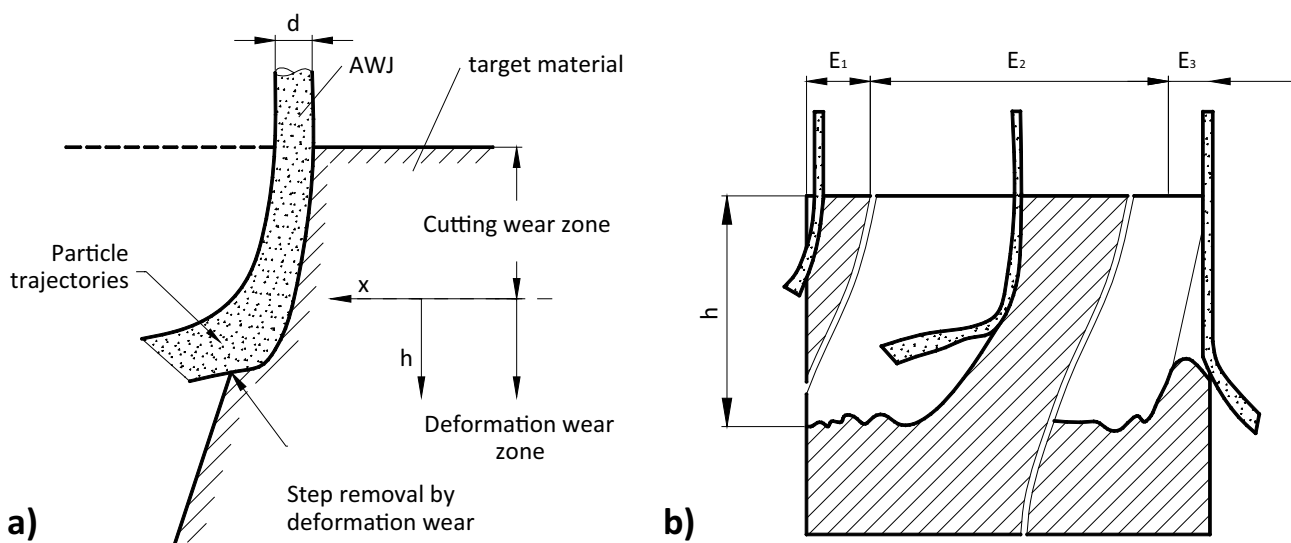

Fig. 1 (**a**) Cutting and deformation mechanisms of wear as designed by Hashish; (**b**) three stages in the cutting process: E1—input stage, E2—stabilized cutting, E3—output stage. (*h*—depth of cut) From [19] (redrawn)

Table 1 Definition of quality levels in [4]

Quality levels Q	Description
1	Criteria for separation cuts. Usually, $Q > 1.2$ should be used
2	Rough surface finish with striation marks on the lower half of the surface
3	Smooth/rough transition criteria. Slight striation marks may appear
4	Striation-free for most engineering materials
5	Very smooth surface finish

test shows that there are two essential phases of material disintegration. During the first phase, the particles hit the surface at a small angle and grind off the material. In the second phase, larger parts are broken from the material as the abrasive particles hit at a steeper angle. According to Hashish, the disintegration process consists of three stages: the input stage, material cutting stage, and output stage. In the cutting zone, material removal is performed by abrasive particles under shallow angles, while in the deformation zone high angles are apparent (Fig. 1b). The erosive process occurs in a cyclic way, with stable material removal until critical depth h_c. Below critical depth h_c, the process of material removal is uneven, causing the formation of striae and waviness of the surface, as per Hashish. A change in the material removal mechanism below the critical depth causes waviness of the cutting material surface. The water in the AWJ serves almost exclusively as a carrier medium, which accelerates the abrasive particles. However, the influence of particle size and properties is not apparent from this publication [3].

Chao et al. [27] studied the connection of striation formation and two-phase cyclic material removal similar to experiments conducted by Hashish [19], proving the cyclic character of the cutting process. Contrary to Hashish, who determined an exact boundary and distance between two removal mechanisms, the result of which is two different types of surface profiles, their findings showed that the formation commenced in the proximity of the surface (Fig. 1). This fact indicated the singularity of the material removal mechanism [23]. They found that the striae begin in the segment on the material surface, unlike the smooth zone considered by Hashish. Lemma et al. [23] investigated mechanisms such as the kinetic energy of abrasive particles and equipment vibrations as causes of unevenness and striation formation. The designed models of striation formation mechanisms in some cases do

not provide an explanation of the erosive entity of AWJ, whereas other models are fundamentally different. Using the model studies summarized by Hashish, Zeng and Kim [28] first investigated the behavior of the abrasive particles during the cutting process and determined the material removal of a single particle. Thus, a first equation was developed, which estimates the cutting depth depending on the cutting speed v_c, the nozzle diameter d, and the abrasive mass flow $\dot{m}_a$ (Eq. 1).
[28]

$$v_c = \left(\frac{N_m * p_w^{1.25} * \dot{m}_w^{0.687} * \dot{m}_a^{0.343}}{8800 * Q * h * d^{0.618}} \right)^{1.15} \left[\text{mm} \middle/ \text{s} \right] \quad (1)$$

where, N_m is the machinability number, p_w is water pressure, m_w is water flow rate. Experiments with various materials and works by other authors have confirmed that the model can be used for all common materials. In order to achieve better practicality and applicability, an equation has been developed from this preparatory work in which the weighting of the individual parameters is carried out by exponents. To determine these exponents, Zeng again carried out a large number of cutting tests with various materials. The values were determined by means of a regression analysis. It was also Zeng who introduced the processing number N_m as a material-specific quantity to classify the material specifically for the AWJ [28]. The definition of quality levels by Zeng is given in Table 1, with examples of the section surfaces in Fig. 2. The user-friendly formula with which the cutting speed can be determined (hereinafter called the Zeng formula) is given as Eq. (1). The parameters nozzle distance, abrasive grain diameter, and abrasive type have no influence on this formula. However, the abrasive type is an important aspect that may have a major influence on the cutting depth and thus on the final cutting speed. This is not explained in more detail by the author [28], but the influence of the

Fig. 2 Samples of the five quality levels [12]
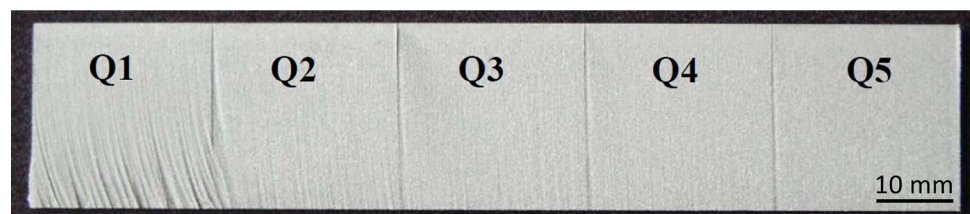
abrasive on the cutting depth is understandable. Round grains, for example, form blunt edges, whereas angular or harder grains remain sharper for longer. Zeng describes the determination of a correction factor, which must be determined individually for each abrasive material pairing.

The Swiss standard 214,001 "Berührungsloses Trennen-Wasserstrahlschneiden-Geometrische Produktspezifikation und Qualität" defines the surface characteristics typical for AWJ such as cutting angle defects (u), edge radius (r_k), ridge (g), groove width (f), striation mark displacement (n), and dimensional and quality tolerances (Fig. 3).

The roughness of the cutting surface is mainly influenced by the cutting speed, material type, and thickness, and to a lesser extent by the cutting medium and process control. According to the roughness definition used here, it can be assumed that the waviness is also partially involved in the roughness. The roughness value R_a is thus a mixed value composed of two different values, which cannot be exactly differentiated. The first size is the basic roughness (microscopic) and is influenced exclusively by the abrasive grain size. This form of surface finish can also be found in sand blasting, where the material removal takes place in the same way as in the AWJ. The second size is the macroscopic waviness [2]. Unfortunately, no classification takes place with regard to the type of surface view, i.e., how the roughness determination has to be carried out (periodic or aperiodic profile, determination of the profile filters). Table 2 lists the five Q levels according to the standard, including a sample image.

Miles and Henning [29] took a closer look at the type of surface measurement. They used the relationship between surface quality and cutting depth created by Zeng. The Zeng formula provides a connection between otherwise constant setting parameters in that the cutting depth is an inverse function of the surface quality defined by the Q levels. Therefore, the present study acknowledges the problem of the subjectivity of the Q levels and develops a method for standard measurement of the surface with profilometers.

Until now, there has been no method developed for the completely clear determination of the surface quality for AWJ surfaces. The quality levels are partly different from each other and insufficiently defined. In all the sources listed above, at least quantitatively, no distinction is made between roughness and waviness. According to the standards DIN EN ISO 4287 and DIN EN ISO 4288 of the surface assessment, the measurements of roughness made in the sources, in which the waviness is incorporated or at least not clearly delimited between the sizes, are prohibited for determination of the surface quality. In addition, all publications lack information about the profile filters and the type of surface, because AWJ-typical surfaces can be viewed either periodically or aperiodically. Therefore, a discussion must take place about a new approach for the better determination of the surface quality by means of striation mark displacement (n), roughness (R), and waviness (W).

Fig. 3 Description of dimensions at the AWJ cutting surface in SN 214,001 [2], where g = ridge, hf = fine cut length, hr = remaining length, r_k = edge radius, sb = jet-influenced zone, t = cutting thickness, u = cutting angle error, f = width of striation marks, n = striation mark displacement, s = water jet entry side
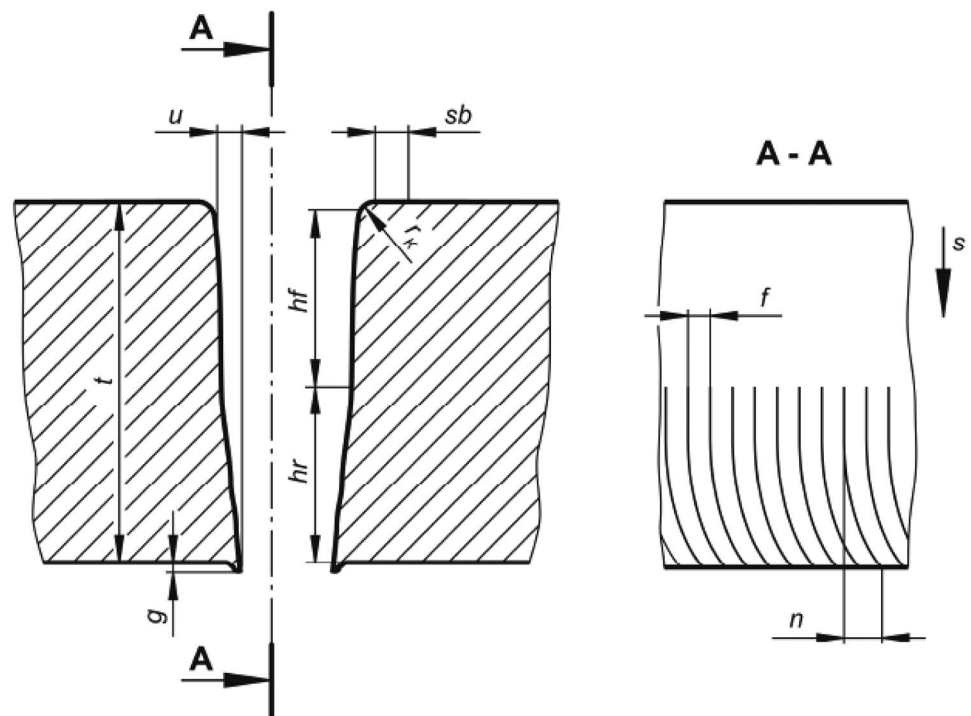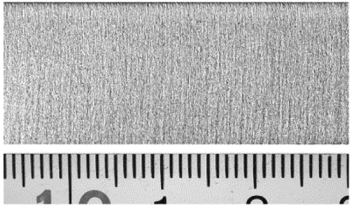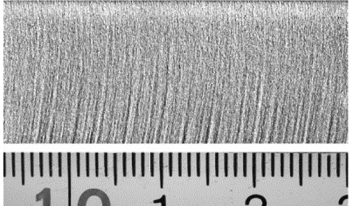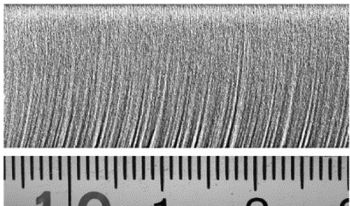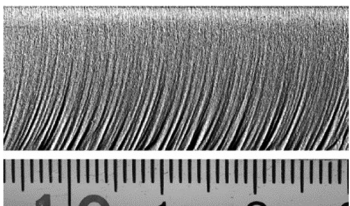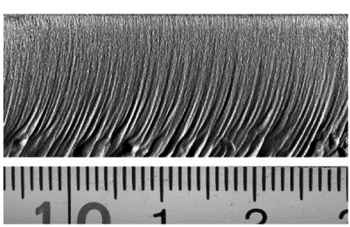
Table 2 Definition of quality levels in [2]

Q level	Description	Cutting surface
Q5	This quality level results in the highest accuracy of the workpiece and the smallest surface roughness. Q5 requires very low traversing speeds. No visible striation marks	
Q4	This quality level is characterized by high accuracy of the workpiece and low surface roughness. Striation marks are slightly visible	
Q3	The usual cut, mostly chosen for economic reasons. It offers good quality and economical feed rates. Striation marks are clearly visible	
Q2	Rough cut with clear but regular striation marks without outbreaks	
Q1	The workpiece was cut at the maximum feed rate. The cutting surface may have significant irregularities (rough striation marks, breakouts, interrupted cuts, washouts, etc.)	

The aim of this work is, therefore, first to extend and concretize the definition of the Q levels in connection with the quantitative determination of the striation mark displacement. By linking these two variables, good applicability and practicality could be achieved. The final goal is thus a quantitative determination of the surface quality without tactile or optical measurements, but purely with the length measurement of the striation mark displacement n (Fig. 3). This measurement can be carried out very quickly with a vernier caliper and is therefore particularly user-friendly during setup or quality control during ongoing operations of the AWJ system. It should be noted that the initial zone is neglected in this study for practical reasons [30].

2 Materials and methods

2.1 Materials

The aim of the selection of sample materials for the current study was to select three materials with different hardness values, which together cover the entire range of materials generally used. In addition, these represent materials that are often machined, so that it can be determine practical reference values from the results obtained. For this reason, the following three materials were used: alloyed tempered steel (50CrMo4 ISO-No: 1.7228), an aluminum alloy (EN AW-5183A), and a polyethylene plastic material (PE-LD

(Trade name Dyneema)). This preselection was helped by a list of different materials and their N_m values, which can be seen in Fig. 4. This presentation enabled an initial estimation of the processing number N_m of the selected test materials. The next step was to determine the true value.

In order to make statements about as many materials and cutting parameters as possible with as few test cuts as possible, the "design of experiments" (DoE) method was used to plan the practical series of runs. The processing characteristics referred to in the following section as "free variable parameters" were combined in a full factorial design in the combination of the four factors (water pressure, machinability number (N_m), abrasive mass flow rate, and quality level) on three levels, with $3^4 = 81$ test runs. The experimental cuts were carried out with the water jet system of the University of Applied Sciences Ulm (Fig. 5). For pressure generation, a high-pressure amplifier (BYPUMP 50APC), was used, with which a maximum working pressure of 400 MPa is possible at a flow rate of 5 l/min. The maximum working area was $1000 \times 1000 \times 400$ mm. An abrasive mixer from the Swiss company Allfi was installed for the feeding of the abrasive-type GMA ClassicCutTM 80 (Mesh 80) [26]. A nozzle with inner diameter $d = 0.28$ mm was used. The diameter of the focusing tube was $d_f = 0.8$ mm. The stand-off distance between the focusing tube and the workpiece was $z = 1$ mm for all cuts. This value has its background in practical applications. A larger distance would lead to a widening of the jet and thus a loss of power density. A smaller distance could cause a collision between the workpiece and nozzle in the event of unevenness of the workpiece support. A sample thickness $b = 15$ mm was kept for all test cuts and for all materials. This facilitated the production of test pieces as well as their evaluation, since the measuring distance for the evaluation of the surface quality was parallel to the workpiece outer edge.

In [8, 32], the influence of the abrasive type is measured on the cutting depth and thus on the cutting speed with a correction factor. Just like N_m, this goes into the Zeng formula without any influence. In this experimental work, the same abrasive material of type GMA ClassicCutTM 80 (Mesh 80) was used. The factor is neglected throughout the work, as under these conditions it only scales the results but has no change in effect related to the materials. The abrasive mass flow rate was adjusted at three levels: 290, 460, and 570 g/min. These values were obtained from the results of the abrasive calibration with 60%, 70%, and 80% of the motor current, as shown in Fig. 6. This covers the usual abrasive quantities in the application.

Since the calculations of traverse speed v_c are based on Zeng's predictive model, the quality level values must be used as variable parameters in this model. The quality levels stipulated by Zeng cover the usual surface qualities for AWJ cutting. The predictive model of this work is intended to cover also the quality range as of Zeng's model, which is why quality levels 5, 3, and 1.2 were tested in the test sections. The dependent variable parameters have a formula-direct dependence on the sizes of the freely variable parameters to be selected. The cutting speed v_c is calculated according to Zeng's feed forecast and depends on the variable values inserted in Eq. (1). The selected nozzle diameter and water pressure determine the water mass flow after taking into account the physical bases with reference to the water density Eq. (2) sets out the context:

[33]

$$\dot{m}_w = v_w * d^2 * \frac{\pi}{4} * \rho_n \quad \left[{}^{kg}/_s \right] \tag{2}$$

A value of 1003 kg/m^3 is assumed to be the normal density of the water. The velocity of the free water jet v_w is determined by the Bernoulli equation:

[33]

$$v_w = \sqrt{\frac{2 * p_w}{\rho_{p_w}}} \quad \left[{}^{m}/_s \right] \tag{3}$$

In this case, the pressure dependence of the density must be considered because of the high working pressure. For 250–500 MPa, i.e., 2500–5000 bar, the following equation applies:

[34]

$$\rho_w(p_w) = -p_w^2 * 10^{-6} + 0.0364 * p_w + 1003 \left[{}^{kg}/_{m^3} \right] \quad p_w in bar \tag{4}$$

To determine the processing number N_m, one must estimate the hardness via Eq. (5):

[31]

$$N_m = \left(\frac{1077}{R_b} \right)^{1.44} \tag{5}$$

The correlation between the Rockwell hardness B and the workability number is used here. Unfortunately, Zeng does not indicate the test requirements or a standard, so for this work the standard Rockwell hardness $HRBW$ with tungsten carbide ball (1.5875-mm diameter) was assumed as the push-in body [35]. According to Zeng, this correlation applies only to metals and is based on the similarity between the materials [12]. Experimentally, the above method of determination was also extended to the polyethylene plastic in this work. The hardness measurements were carried out on a ZwickRoell universal hardness tester ZHU250 top (ZwickRoell Pvt. Ltd. CIPET Industrial Estate, Chennai, India). At the time of the test, there was no possibility of determining the hardness in $HRBW$, so the Brinell hardness HB was used for the determination.
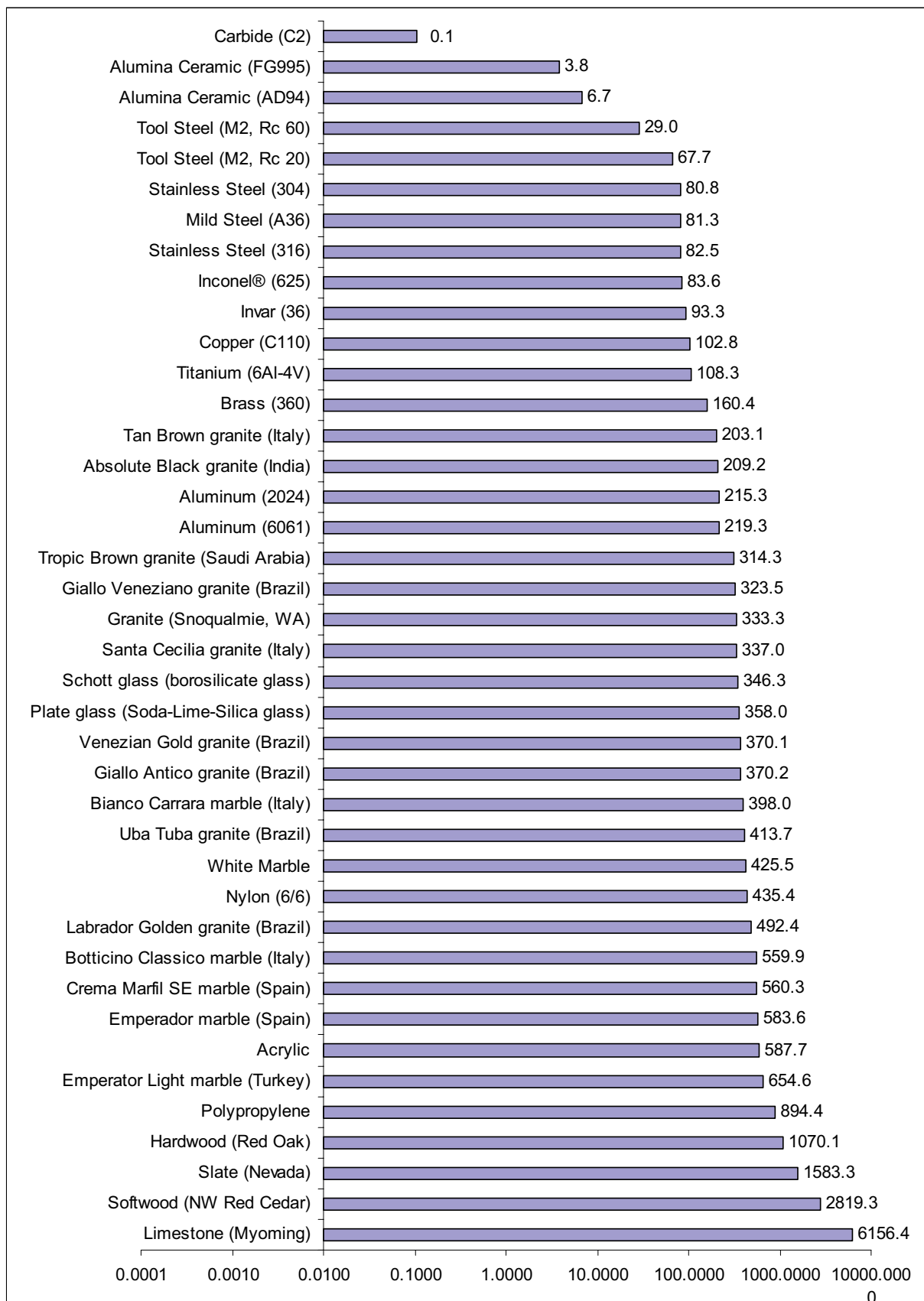
Material	Value
Carbide (C2)	0.1
Alumina Ceramic (FG995)	3.8
Alumina Ceramic (AD94)	6.7
Tool Steel (M2, Rc 60)	29.0
Tool Steel (M2, Rc 20)	67.7
Stainless Steel (304)	80.8
Mild Steel (A36)	81.3
Stainless Steel (316)	82.5
Inconel® (625)	83.6
Invar (36)	93.3
Copper (C110)	102.8
Titanium (6Al-4V)	108.3
Brass (360)	160.4
Tan Brown granite (Italy)	203.1
Absolute Black granite (India)	209.2
Aluminum (2024)	215.3
Aluminum (6061)	219.3
Tropic Brown granite (Saudi Arabia)	314.3
Giallo Veneziano granite (Brazil)	323.5
Granite (Snoqualmie, WA)	333.3
Santa Cecilia granite (Italy)	337.0
Schott glass (borosilicate glass)	346.3
Plate glass (Soda-Lime-Silica glass)	358.0
Venezian Gold granite (Brazil)	370.1
Giallo Antico granite (Brazil)	370.2
Bianco Carrara marble (Italy)	398.0
Uba Tuba granite (Brazil)	413.7
White Marble	425.5
Nylon (6/6)	435.4
Labrador Golden granite (Brazil)	492.4
Botticino Classico marble (Italy)	559.9
Crema Marfil SE marble (Spain)	560.3
Emperador marble (Spain)	583.6
Acrylic	587.7
Emperator Light marble (Turkey)	654.6
Polypropylene	894.4
Hardwood (Red Oak)	1070.1
Slate (Nevada)	1583.3
Softwood (NW Red Cedar)	2819.3
Limestone (Myoming)	6156.4

x-axis: 0.0001 0.0010 0.0100 0.1000 1.0000 10.0000 100.0000 1000.0000 10000.0000

Fig. 4 List of materials and their machinability [31]
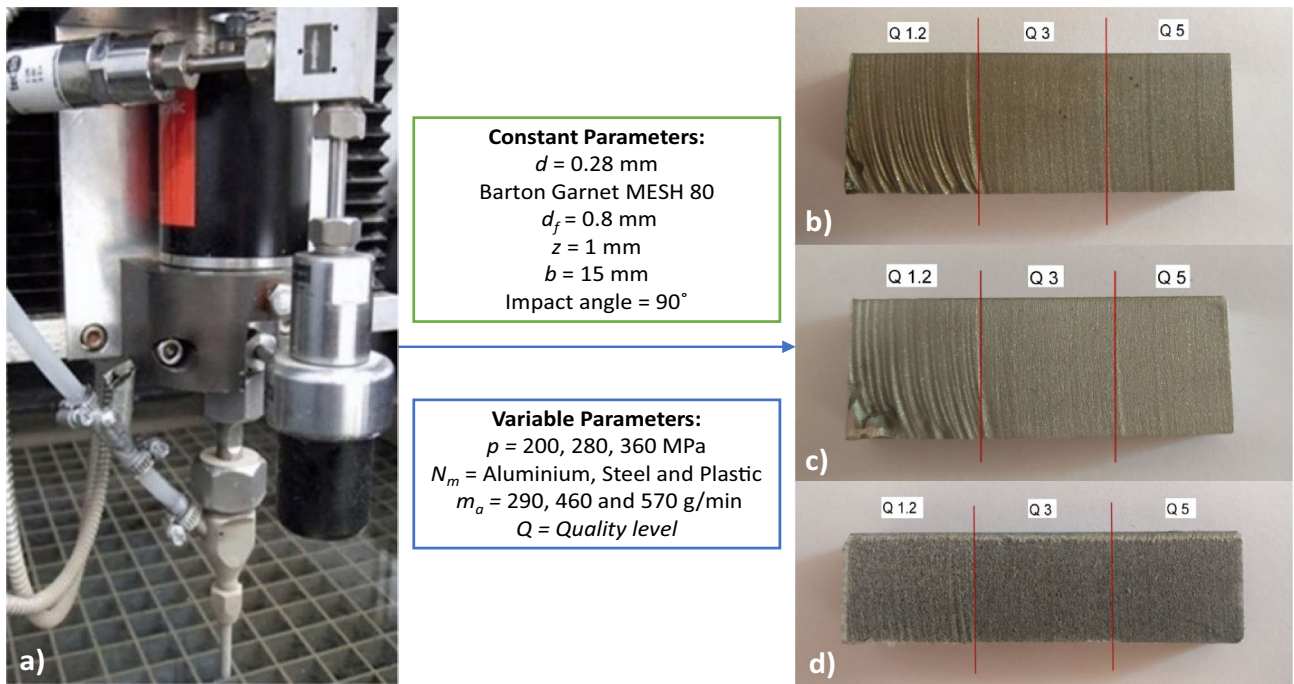
Fig. 5 Experimental setup: (**a**) a cutting head, (**b**) stainless steel 50CrMo4—308 HRBW, (**c**) aluminum alloy EN AW-5183A—77.4 HRBW, (**d**) polyethylene plastic—97.5 HRBW

A tungsten carbide ball with a diameter of 2.5 mm was used as the test specimen, and the ball calotte was evaluated after [36]. The measured values were revalued after [37]. For the tempered steel, after interpolation, a value of 108 HB was determined, with a value of 34 HB for the aluminum. For aluminum, the result is critical, because the validity of the revalued table has a wide range and it could not be clarified whether the aluminum used here fell within this range. The calculation of the machinability number results in values of $N_m = 27$ for steel and $N_m = 147$ for aluminum. No value can be determined for polyethylene plastics, since the measured shore hardness cannot be converted into a Rockwell hardness due to the difference in the materials. For this reason, the determination of N_m for polyethylene plastics is not possible and must therefore be performed differently. The second investigation procedure, which does not require a reference material with known machinability, is based on the following idea. The Zeng formula (Eq. (1)) is converted to N_m, resulting in the following connection:

Fig. 6 Calibration of the abrasive mass flow rate
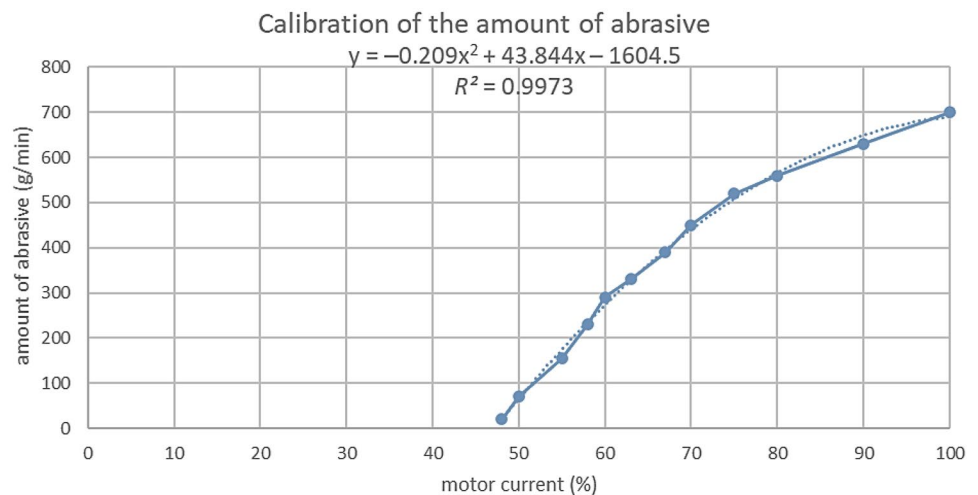
$$N_m = \frac{8800 * h * d^{0.618} * v_c^{0.866} * Q}{p_w^{1.25} * \dot{m}_w^{0.687} * \dot{m}_a^{0.343}} \quad [-].\qquad(6)$$

Choosing values based on experience or appropriate tables, we first selected a cutting speed. The quality level Q was set to 1.2 to obtain a safe cut (Table 1). With this setting, a wedge-shaped workpiece was cut, which consisted of the material to be determined. The maximum penetration height in the test wedge now represented the missing size h for N_m determination and was measured. For the materials used in these tests, the results were, for steel, $N_m = 21.8$; for aluminum, $N_m = 60.5$; and for polyethylene plastic, $N_m = 100.1$. These values were then used for testing and evaluation.

2.2 Measurement

The measurement of the surface characteristics in the cutting surface was carried out with a contour- and roughness-measuring device (Zeiss Surfcom 1900SD). The surface roughness profile parameters R_z and R_a were determined in accordance with DIN EN ISO 4287 [38] and DIN EN ISO 4288 [39]. R_z is sum of maximum peak height and valley depth within the evaluation length. By measuring the RSm value at the cutting outlet of an exemplary sample, the boundary wavelength of λ_c was first determined to be 2.5 mm. This resulted in a single measuring distance l_r of 2.5 mm and a measuring distance l_n of 12.5 mm, based on [39]. The lower wavelength was set by the filter λ_s to 8 μm. After checking the recorded primary profile curve and the roughness curve after filtering with the above filter values, a clear representation of the ripple in the roughness profile showed that a significant proportion of the ripple was still included in the roughness value. For this reason, the filter λ_c was subsequently reduced to 0.25 mm for all samples until no ripple was visible. Only in this way could a clear separation be made between roughness and ripple. W_z was determined as the maximum depth of waviness within the evaluation length according to DIN EN ISO 4288 [39]. The position at which the measurement is carried out on the sample cutting surface is specified in the Swiss standard SN 214,001 [40]. According to this, the measurement must be carried out in the lower 10% of the cutting surface, but at least 1 mm from the lower edge. In this evaluation, due to the cutting depth of 15 mm, it was measured parallel to the lower edge, 1.3 mm away from it.

The striation mark displacement n was determined with two different microscopes. For samples that showed a strongly pronounced striation mark displacement as well as a large ripple in the cutting surface, the Mitutoyo Vision Measuring Machine QS250Z was used. If the striation mark displacement was impossible or difficult to detect with this measuring device, the Olympus SZX12 stereo microscope was used for a better exposure capability of the sample. The striation mark displacement n was measured according to the Swiss standard SN 214,001, as shown in the cutaway diagram A-A in Fig. 3.

With the software of the respective microscopes, the beginning of a striation mark was marked with a line perpendicular to the workpiece surface. The water jet outlet was marked with a second line parallel to the first. The distance between the two lines gave the striation mark displacement n. Three representative striation marks were measured on each sample, and their mean value was calculated. If no striation mark displacement was recognizable, it was rated 0.

3 Results and discussion

For the determination of the results, the usual roughness characteristics R_z (average roughness depth), R_a (arithmetic center roughness), and the highest height of the roughness Rt were measured. The values for the ripple W_z as well as the sizes Pz, Pa, and Pt of the primary profile were measured. By experimentally compiling different diagrams, a comparison and evaluation of the surface characteristics were carried out. In the case of AWJ, larger depressions or marks were produced at irregular intervals, e.g., due to a short-term abrasive quantity maximum due to discontinuous mixing. Therefore, the maximum roughness Rt is not a representative quantity. The characteristic values of the primary profile without filtering seem reasonable and probably also correspond to the so-called roughness values of some of the above-mentioned sources, in which the ripple flows into the roughness. However, these variables play a minor role in practice and are therefore not effective here. The remaining surface characteristics R_z, R_a, and W_z, however, are more practical and are therefore explained in more detail below. In the case of polyethylene plastics, measurable striation mark displacement only occurred in a few cases. The majority of the samples showed a rough surface with barely visible or invisible striation marks. Therefore, there are no useful diagrams for polyethylene plastic from which conclusions can be drawn in comparison to harder materials such as steel and aluminum.

3.1 Roughness, R_z, as a surface characteristic for AWJ cutting

Figures 7 and 8 show the striation mark displacement n and the average roughness R_z for the aluminum and steel samples, respectively with a nozzle diameter of $d = 0.28$ mm. The results were divided according to quality levels and are presented with a balancing straight line for each Q level. It can be seen that measuring the striation mark displacement alone does not give an idea of the roughness. This is
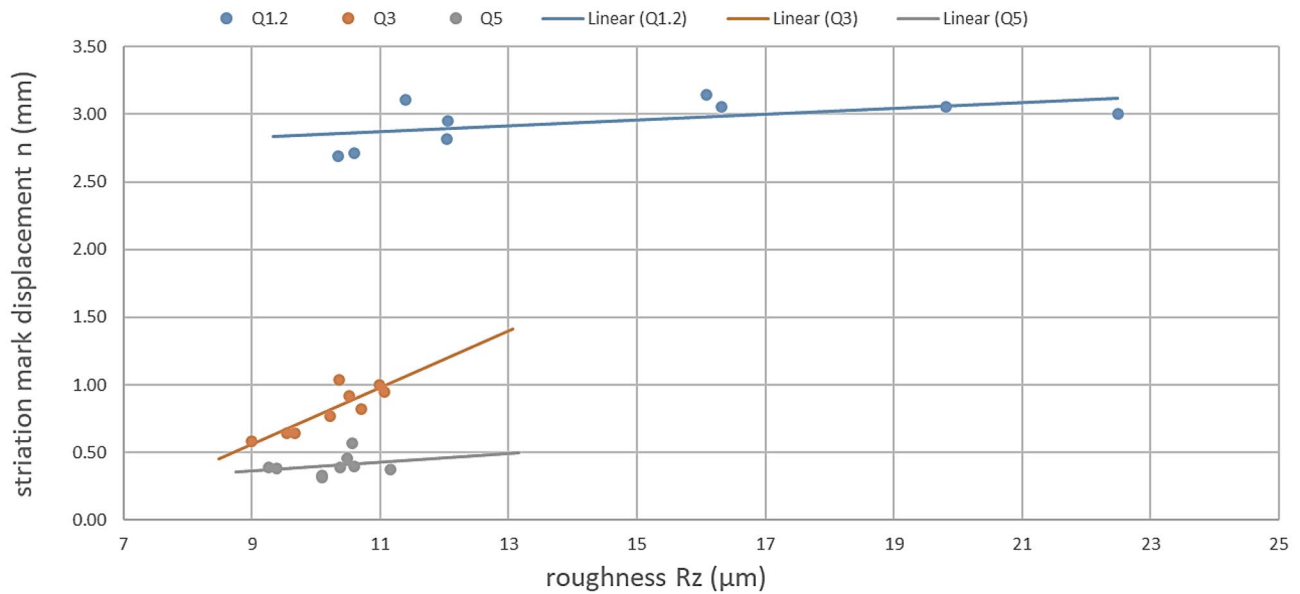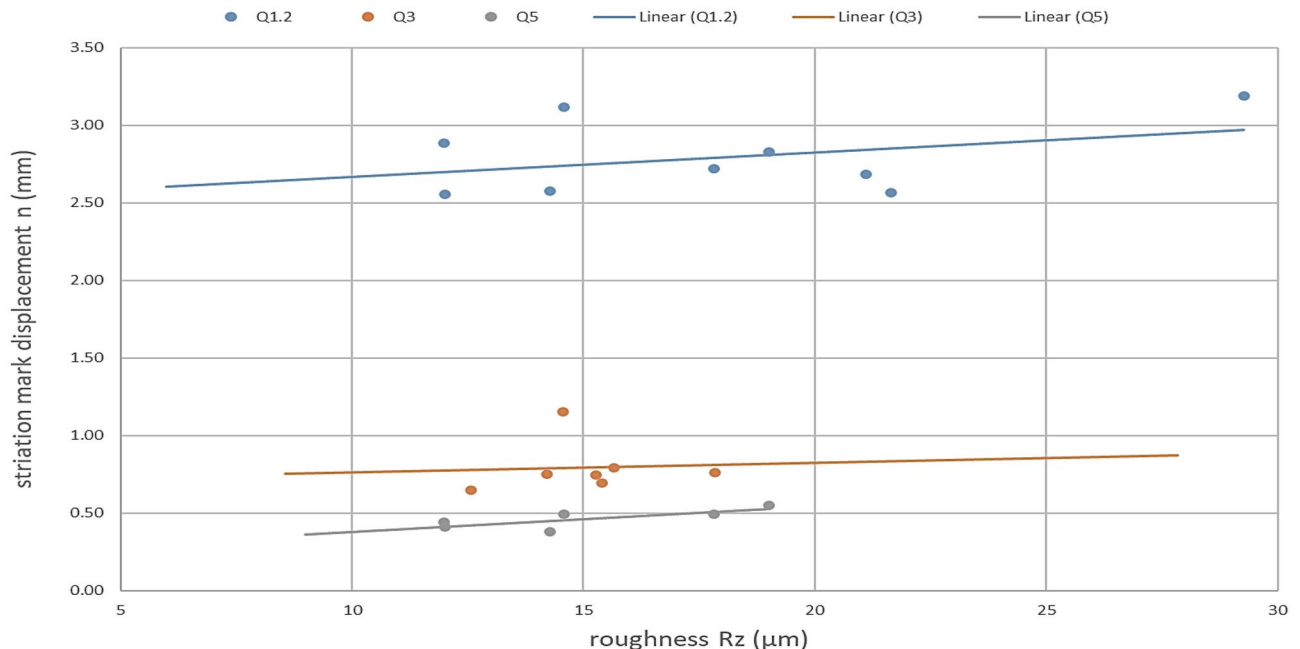
Fig. 7 Correlation between striation mark displacement and roughness R_z for single Q levels. (Steel) (N_m=21.8, p_w=200–360 MPa, m_a=4.8–9.5 g/s, GMA 80, d=0.28 mm, d_f=0.8 mm, s=1 mm, h=15 mm)

the case for all materials: for steel, the indistinct range of roughness is 9–12 μm. The striation mark displacement in this relatively small span of roughness varies between 0.11 and 3.11 mm. Even with knowledge of the Q level of the cut, the roughness cannot be clearly determined. The reason for this is the low variance of the striation mark displacement over the roughness as well as the large dispersion of the values. This observation confirms the assumption that roughness depends mainly on the abrasive grain size and material,

rather than on the cutting parameters. Figure 9 confirms this observation by an evaluation of the DoE with Minitab software (Minitab LLC, state college, PA, USA). The main effect on the roughness is the material-dependent processing rate. The cutting parameter pressure and especially the abrasive quantity have only a small influence in comparison.

Figure 10 shows the relationship between roughness R_z and Q levels for the polyethylene plastic material. If the quality level is known, the roughness can be

Fig. 8 Correlation between striation mark displacement and roughness R_z for single Q levels. (Aluminum) (N_m=60.5, p_w=200–360 MPa, m_a=4.8–9.5 g/s, GMA 80, d=0.28 mm, d_f=0.8 mm, s=1 mm, h=15 mm)
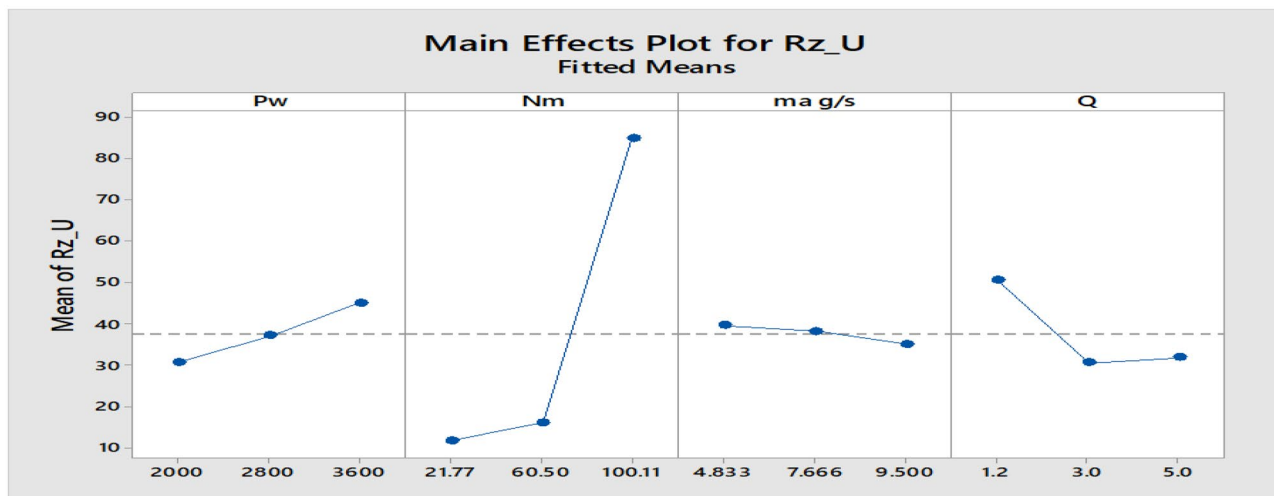
Fig. 9 Main effects and interaction plot for R_z

reliably determined by this graph. However, the correlation between the Q levels and the striation mark displacement would have to be known for this. Since the striation mark displacement with measuring instruments established in the industry could not be determined at $Q > 1.2$, therefore no conclusion can be drawn.

3.2 Roughness R_a as surface characteristic for AWJ cutting

Figures 11 and 12 show the striation mark displacement n and the center roughness R_a for the aluminum and steel samples, respectively. The results were divided according
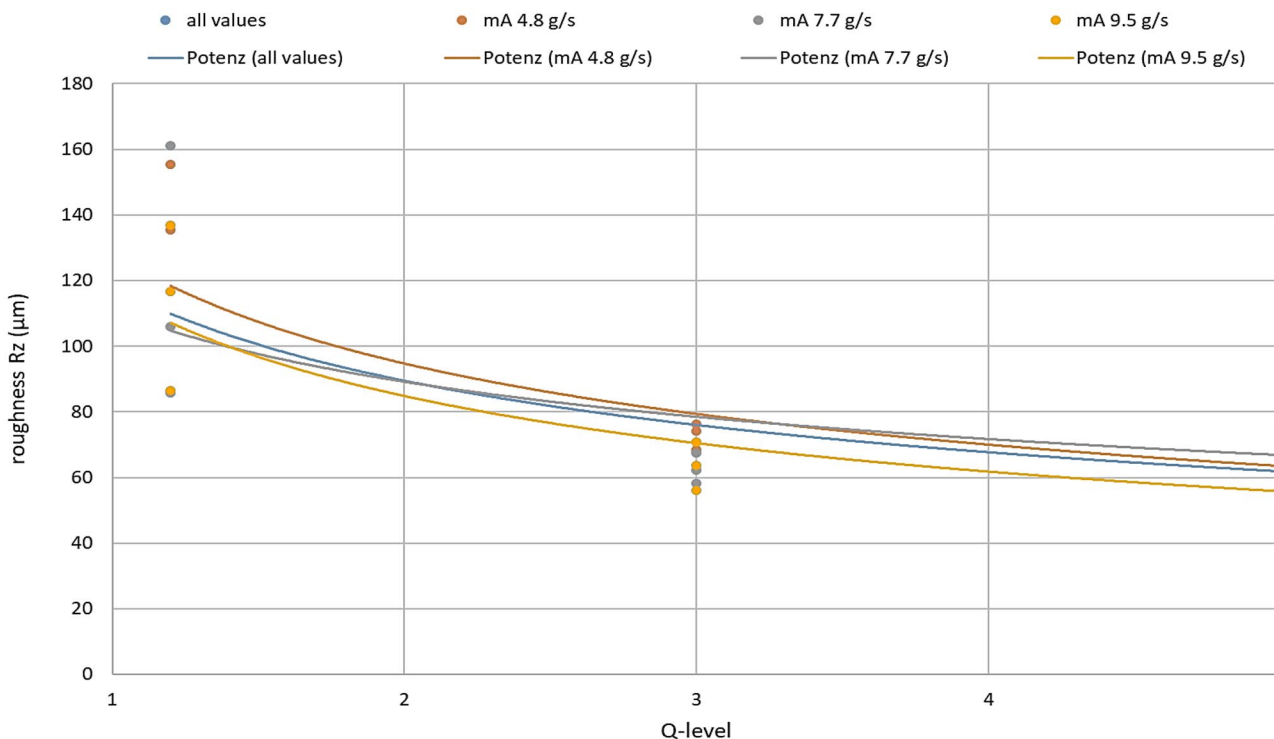
Fig. 10 Correlation between roughness R_z and Q level for polyethylene plastic. ($N_m = 100$, $p_w = 200$–360 MPa, $m_a = 4.8$–9.5 g/s, GMA 80, $d = 0.28$ mm, $d_f = 0.8$ mm, $s = 1$ mm, $h = 15$ mm)
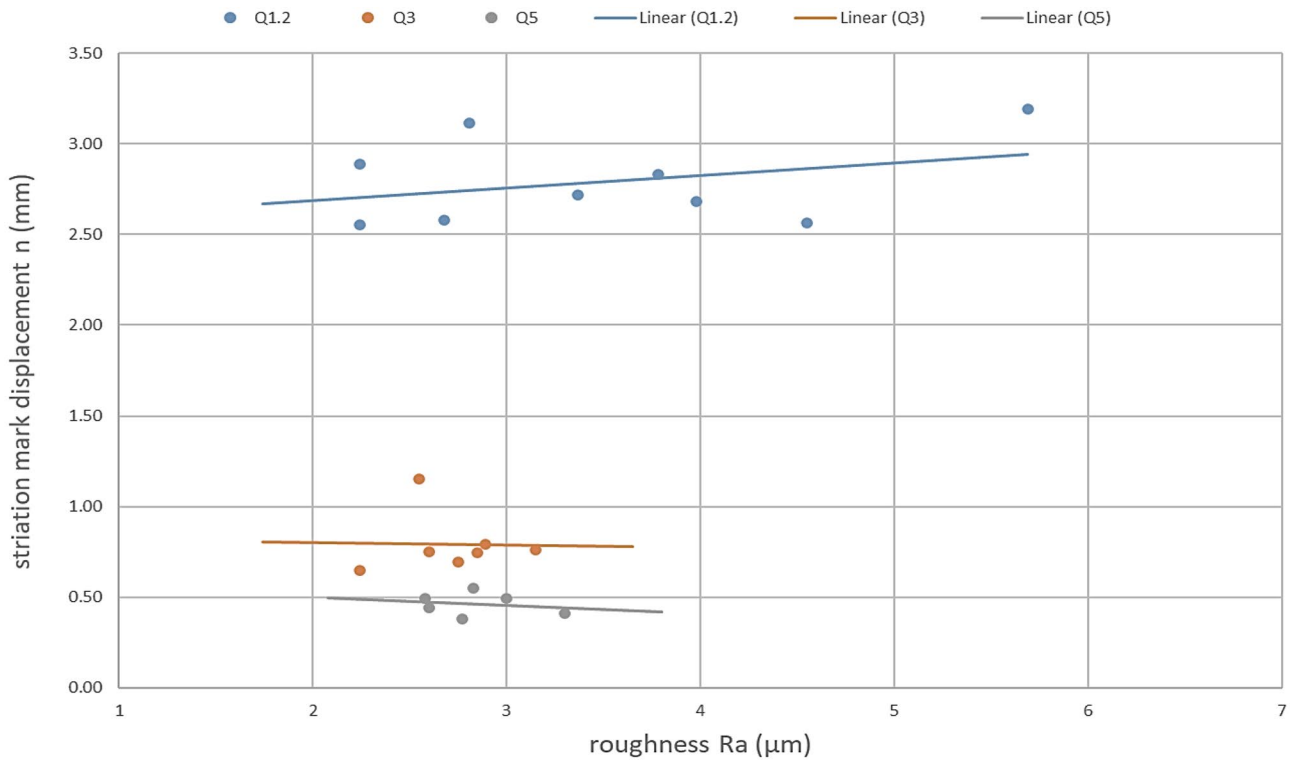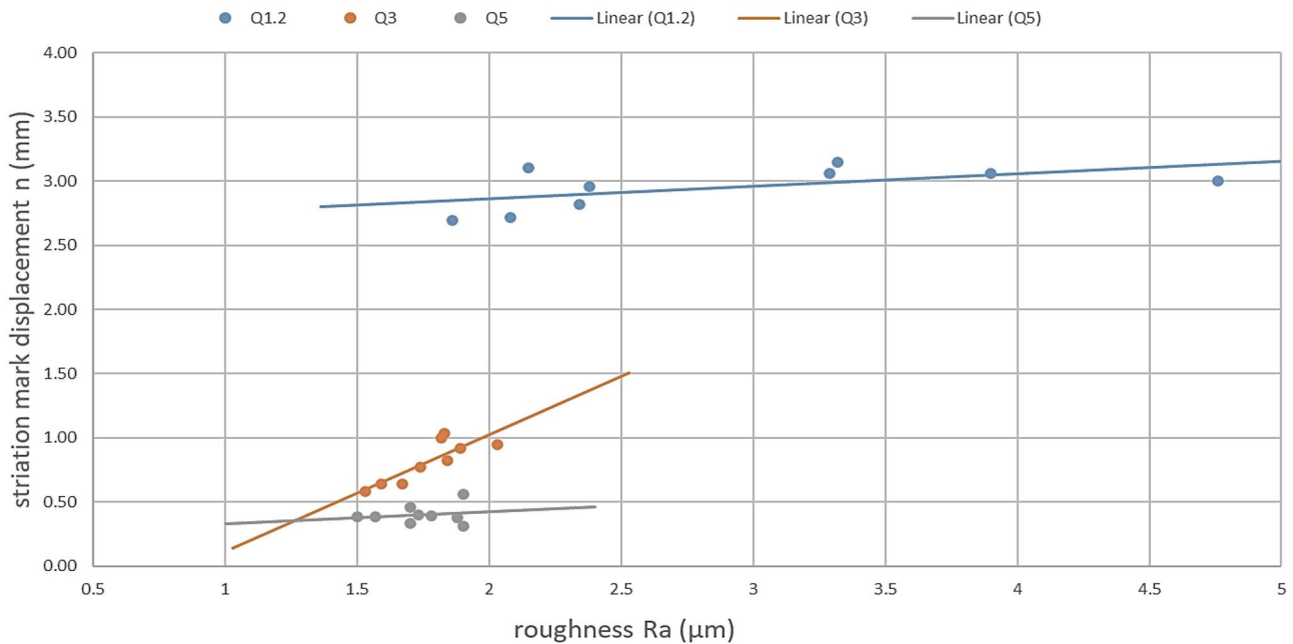
Fig. 11 Correlation between striation mark displacement and roughness R_a for single Q levels (Aluminum). ($N_m=60.5$, $p_w=200$–360 MPa, $m_a=4.8$–9.5 g/s, GMA 80, $d=0.28$ mm, $d_f=0.8$ mm, $s=1$ mm, $h=15$ mm)

to the quality levels Q and are presented with a balancing straight line for each Q level. The surface roughness profile parameter R_a cannot be inferred from measuring the striation mark displacement alone. According to [38], this arithmetic mid-rough value describes the arithmetic mean of the ordinate values $Z(x)$ within a single measurement distance. It

Fig. 12 Correlation between striation mark displacement and roughness R_a for single Q levels (steel). ($N_m=21.8$, $p_w=200$–360 MPa, $m_a=4.8$–9.5 g/s, GMA 80, $d=0.28$ mm, $d_f=0.8$ mm, $s=1$ mm, $h=15$ mm)
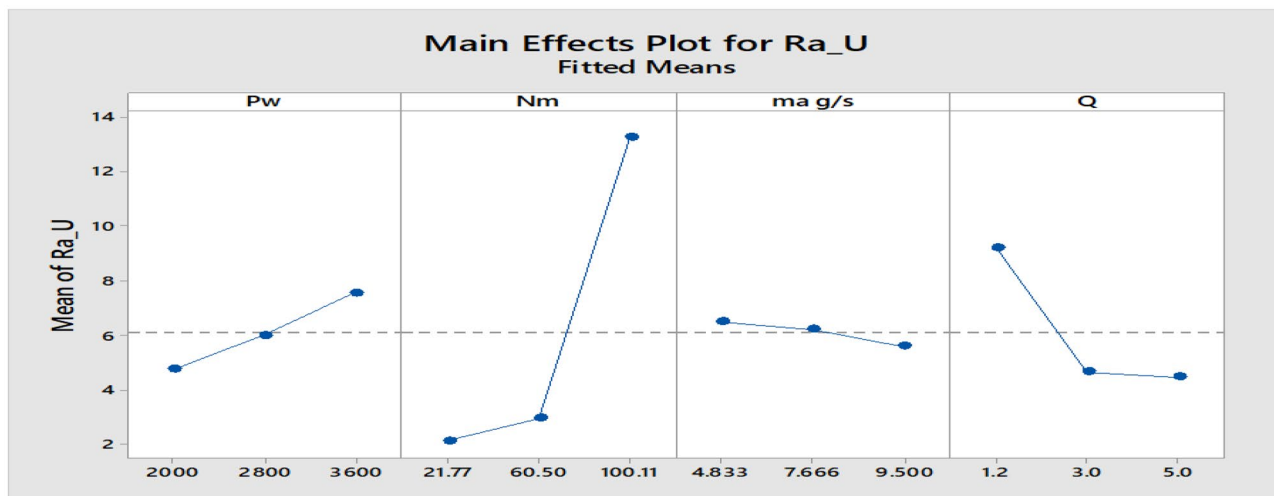
Fig. 13 Main effects and Interaction plot for R_a

is therefore a view of the area. From a purely hypothetical point of view, a measured distance with a single very wide and flat striation mark can therefore have the same value for R_a as an equally long measured distance with a narrow and deep striation mark and otherwise no elevations above the profile center line. This measured value is therefore no longer related to elevation and deepening so that, if the value is considered alone without knowledge of the true profile, no inference can be drawn as to the approximate depth of the surveys. For this reason, the surface characteristic R_a must be regarded as critical, especially in the case of the AWJ. It should also be noted that there is a relatively large statistical variation in the roughness. However, because this size is the most widely used in general mechanical engineering, it must not be neglected and will be discussed further below. The abovementioned effect of the arithmetic surface evaluation is amplified in the ripple, since here the typical striation marks resulting from the AWJ for small Q values are included, which diminishes the effect of both. Therefore, the ripple is considered only with W_z and not with Wa. The negative slope of the balancing straight in aluminum is an illogical relationship and does not fit the general understanding of the surface finish and the origin of it. The different samples of a quality level are so close together that the measurement inaccuracy is greater than the change in roughness due to the different cutting parameter settings. This is further proof
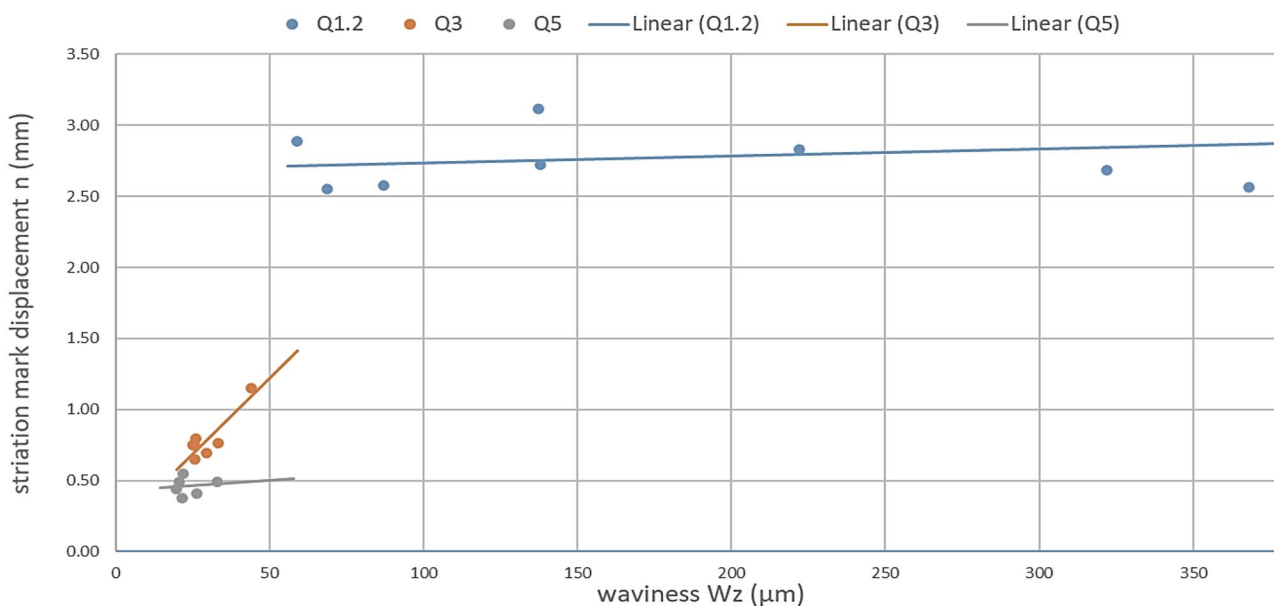

Fig. 14 Correlation between striation mark displacement and waviness W_z for single Q levels (aluminum). ($N_m = 60.5$, $p_w = 200$–360 MPa, $m_a = 4.8$–9.5 g/s, GMA 80, $d = 0.28$ mm, $d_f = 0.8$ mm, $s = 1$ mm, $h = 15$ mm)

that the roughness value R_a is unsuitable for determining the surface quality in the AWJ.

Figure 13 shows that the main effects of R_a are very similar to those of R_z.

3.3 Relationship between striation mark displacement n and ripple W_z

Figures 14 and 15 show the striation mark displacement n above the ripple W_z for aluminum and steel, broken down by the individual Q levels. Here, the connection between the sizes can be clearly seen. With increasing striation mark displacement, a greater striation mark depth is involved, which flows directly into the ripple. This is proof that, for small values for Q, a view of the ripple is more useful than that of roughness. The following evaluation of the main effects on the ripple (Fig. 16) shows this again clearly. The smaller the Q level, the higher its influence on the ripple.

3.4 Influence of the view of the surface as a periodic or aperiodic profile

For a clear standard-compliant determination of surface characteristics, an assignment of the considered surface with respect to their periodicity is necessary. The type of viewing, as shown in Fig. 16, clearly determines the filter settings and thus the boundary between ripple and roughness. In the case of the AWJ, the classification is ambiguous without any further information because, depending on the set cutting parameters, very different surface structures are created. This problem is referred to in the statements made in the Introduction regarding the inaccurate or missing separation between roughness and ripple in the sources.

In this study, the AWJ cutting surface is basically treated as a periodic profile. The reason for this can be found in the ideal hypothesis of the AWJ. The hypothesis assumes that each abrasive grain has a specific time interval in which the material removal takes place. If these intervals are equal in length and lined up, the feed results in regularly recurring striation marks. The distance between these striation marks then varies based on the operating parameters and is called the *RSm* value. Figure 17 shows the history of the *RSm* value over Q for all materials. The measurement was made at the incision, as the surface was approaching the idealization described above. The curves are more qualitative, since only individual sample values have been determined. The colored horizontal boundaries show the limits at which the filter settings must be changed.

At these limits, the proportion of surface finish to which either roughness or ripple must be assigned is changed abruptly. As a result, the requirements for a surface must also be different in each area, since two quantitatively identical values from different ranges differ qualitatively. In order to assign a surface formed by water abrasion blasting by means of the roughness characteristics R_z and R_a to one of the Q levels, no significant striation marks may be present
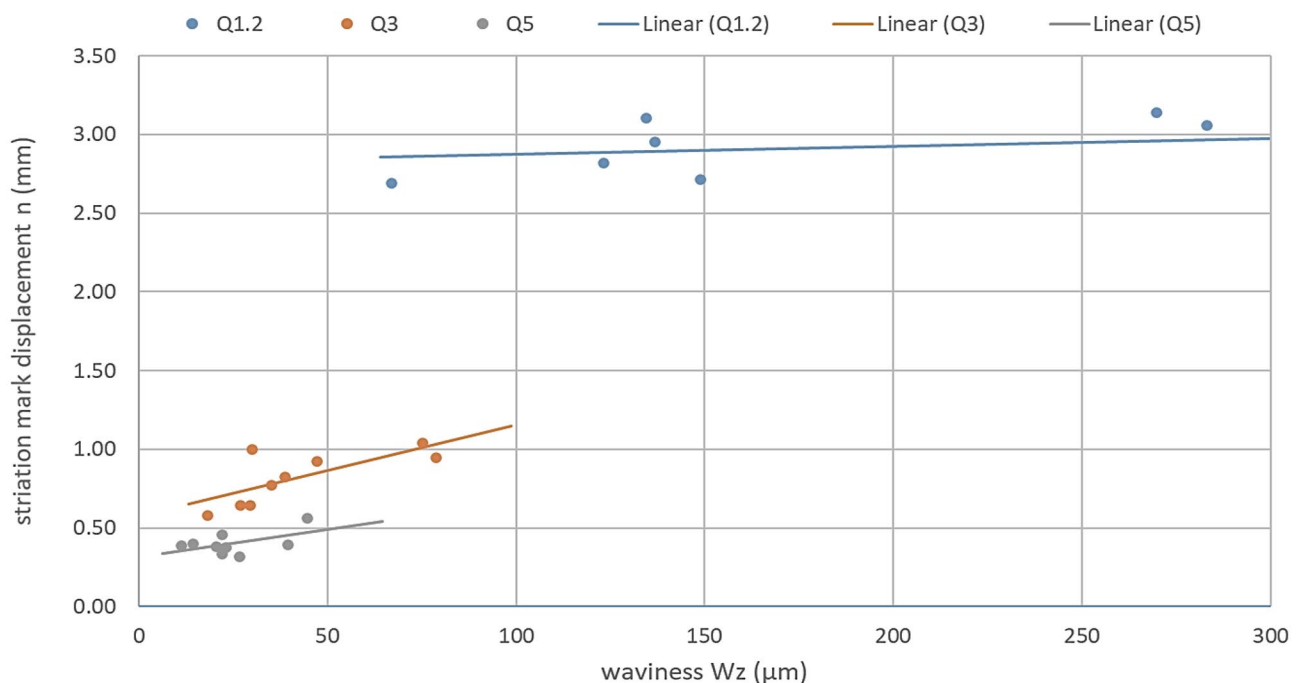

Fig. 15 Correlation between striation mark displacement and waviness W_z for single Q levels (steel). ($N_m = 21.8$–100, $p_w = 200$–360 MPa, $m_a = 4.8$–9.5 g/s, GMA 80, $d = 0.28$ mm, $d_f = 0.8$ mm, $s = 1$ mm, $h = 15$ mm)

Fig. 16 Selection of sampling length and cutoff in accordance with ISO 4288 (04/98) [39]

Periodic profiles	Aperiodic profiles		Cutoff	Sampling length (lr) Evaluation length (ln)
All R parameters and RSm for all profiles	Rz, Rmax, Rt, Rv, Rp, Rc	Ra, Rq, Rsk, Rku, RΔq		
Rsm(mm)	Rz Rmax (µm)	Ra (µm)	Λc (mm)	Lr/ln (mm)
>0.013 to 0.04	>0.025 to 0.1	>0.006 to 0.02	0.08	0.08/0.4
>0.04 to 0.13	>0.1 to 0.5	>0.02 to 0.1	0.25	0.25/1.25
>0.13 to 0.4	>0.5 yo 10	>0.1 to 2	0.8	0.8/4.0
>0.4 to 1.3	>10 to 50	>2 to 10	2.5	2.5/12.5
>1.3 to 4	>50 to 200	>10 to 80	8.0	8.0/40

on the surface. These must be considered as ripple (W_z) and incorrectly influence the measurement of R_z and R_a. For the test series created here, it can be said that the roughness characteristics R_z and R_a can be applied to classify quality levels Q3–5. However, this delimitation of the categorizability of a surface is material-dependent and therefore not fully valid for other materials. There are overlaps here, so in some cases a roughness value can be assigned to all five Q levels. Thus, it can be problematic to define the Q levels only by a roughness value, as can be seen in Figs. 7 and 12. For steel, however, it can be said in this case that above 12 µm the Q level can be clearly determined, namely to Q1.2. If the measured striation mark is then compared to that in the chart in Fig. 7, the roughness value can be considered valid. However, the reference to the filter setting must be made here again. The samples of this work were evaluated at the

beam outlet, contrary to the valid standards, all with the same filter setting described above, in order to ensure better comparability. If the surface is evaluated separately according to ripple and roughness, as in this work, then it turns out that the ripple W_z is better suited for determining the surface. The classification into Q levels can be carried out safely due to the typical striation marks for the AWJ, especially in the rough range by this characteristic value. However, it can be seen in Figs. 14 and 15 that overlaps also occur here. This observation can be attributed to the absence of grooves at the fine Q levels. Therefore, the exclusive measurement of W_z is not a perfect method for surface determination, since only with an undulating surface can a ripple value be determined. The example images from [40] and [29] show a clear increase in the striation mark displacement with a decreasing Q level. Although the description of the sample images
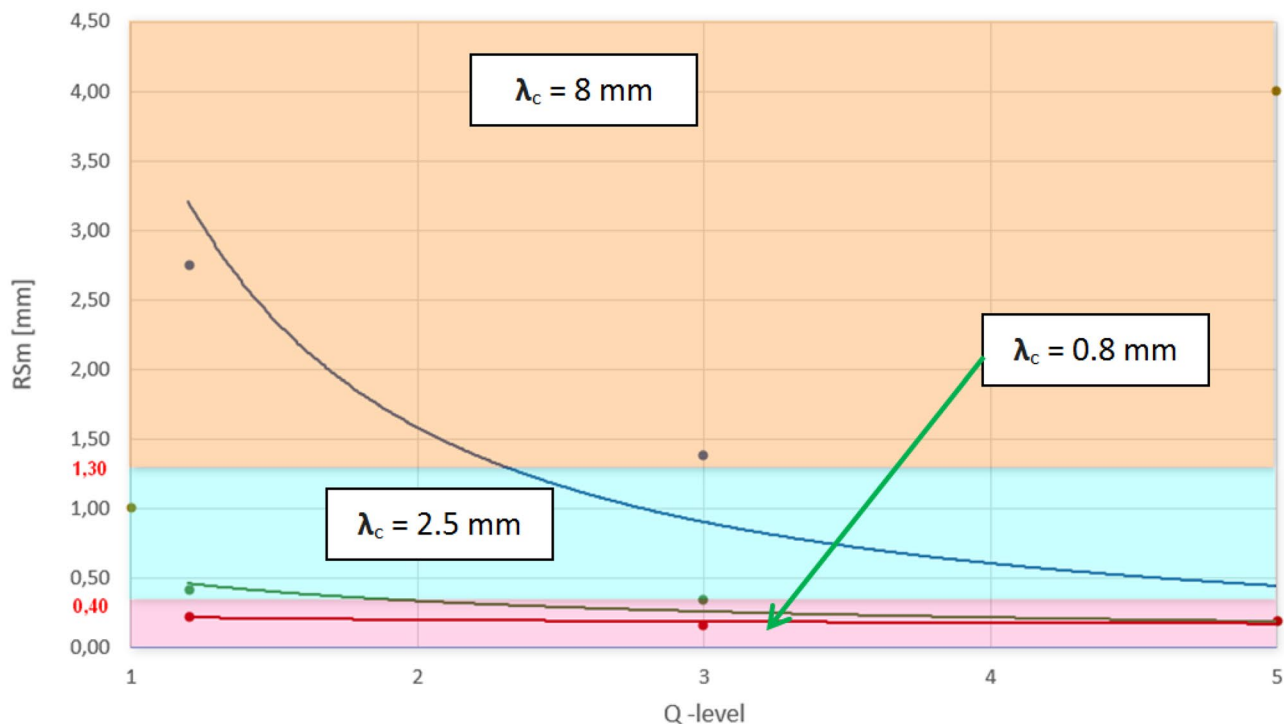

Fig. 17 Correlation between RSm and Q level for all materials. ($N_m = 21.8$–100, $p_w = 200$–360 MPa, $m_a = 4.8$ g/s, GMA 80, $d = 0.28$ mm, $d_f = 0.8$ mm, $s = 1$ mm, $h = 15$ mm)

Table 3 Concrete values of striation marks for single Q levels (steel) with roughness limits

	Q1	Q2	Q3	Q4	Q5
n (mm)	$n > 2.1$	$2.1 \geq n > 1.0$	$1.0 \geq n > 0.7$	$0.7 \geq n > 0.5$	$0.5 \geq n$
R_z (µm)	10–23	9.5–10.8	9–11.5	9.1–11.5	9.2–11.5
R_a (µm)	1.8–4.8	1.7–3.5	1.6–2.1	1.5–2	1.5–1.9
W_z (µm)	> 60	40–100	20–80	15–62.5	10–45

Table 4 Concrete values of striation marks for single Q levels (aluminum) with roughness limits

	Q1	Q2	Q3	Q4	Q5
n (mm)	$n > 2.0$	$2.0 \geq n > 1.1$	$1.1 \geq n > 0.7$	$0.7 \geq n > 0.5$	$0.5 \geq n$
R_z (µm)	12–29	12.5–23.5	13–18	12.5–18.5	12–19
R_a (µm)	2.2–6	2.2–4.6	2.2–3.2	2.3–3.3	2.5–3.3
W_z (µm)	> 50	37–57	25–45	20–38	15–30

Table 5 Concrete values of striation marks for single Q levels (polyethylene plastic) with roughness limits

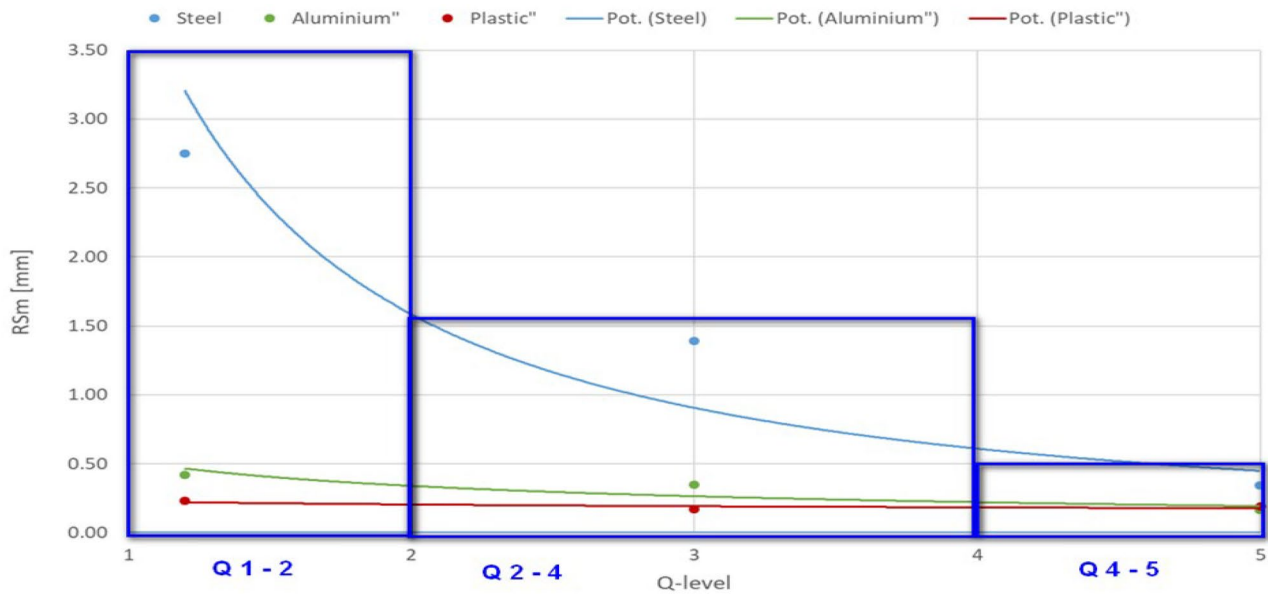|	Q1	Q2	Q3	Q4	Q5
n (mm)	$n > 0.85$	$0.5 \geq n > 0.85$	Incapable of measurement	Incapable of measurement	Incapable of measurement
R_z (µm)	100–120	80–100	70–80	60–70	55–60
R_a (mm)	15–20	12–15	10–12	8–10	7–8

Fig. 18 Correlation between *RSm* and *Q* level for all materials (exemplary) with areas. ($N_m = 21.8$–100, $p_w = 200$–360 MPa, $m_a = 4.8$ g/s, GMA 80, $d = 0.28$ mm, $d_f = 0.8$ mm, $s = 1$ mm, $h = 15$ mm). Area 1 (left) has three values for λc, area 2 (middle) only 0.8 and 2.5 mm, and area 3 (right) only 0.8 mm, if the relationship from Fig. 15 applies to *RSm* and λc. The proposal is therefore as follows. In area 1, i.e., for required surfaces of poor Q2, measuring the striation mark displacement is sufficient to be able to assign the surface without any doubt. In addition, roughness is not important for these poor surfaces, as further processing usually follows. In area 2, i.e., from Q2 to Q4, the roughness becomes functionally important and must therefore be checked in addition to the striation mark displacement. The striation mark displacement must not exceed a certain level, and the roughness should not fall below a limit value, so as not to be unnecessarily expensive. If one of the highest quality levels, Q4 or Q5, is required, then a roughness measurement and a controlling ripple measurement, which must not exceed a certain value, are sufficient, since no or very few striation marks occur. In addition, it must be said that the above tables apply only in one direction because of an R_a value; no inference from the table to the striation mark displacement or the Q level is possible. In this work, tables were created for three representative materials. This publication therefore demonstrates an improved method to categorize the quality of the finished surfaces. According to this procedure, such tables can also be created for other materials or groups of materials with similar physical properties to check the quality. These must also be provided with statistical security. The approach proposed here could make it safer and faster to determine the surface without misunderstandings

refers only to the striation marks and not to *n*, a clear correlation can be assumed qualitatively, independent of the cutting parameters. This assumption is confirmed by the clear relationship between the striation mark displacement and the *Q* levels (Fig. 7). Thus, the striation mark displacement is an easy value to measure when it comes to the unique assignment of a cutting surface to one of the five *Q* levels. However, there is also a problem here. With the finer *Q* levels, no striation mark displacement is measurable or it is equal to 0. In addition, the material used also plays a major role, so softer materials are produced; here, it was polyethylene plastic, often even with coarser *Q* levels and a rather rough surface on which no striation mark displacement occurred. Therefore, in practice, several parameters are always necessary for a clear definition and determination. The following describes how this can be implemented for practical applicability (Tables 3, 4, and 5).

4 Conclusions

The following recommendations for the categorization of AWJ surfaces should help to objectively check the manufactured surface for the required *Q* level in practical applications. Furthermore, it is possible to assign the surface to a range of surface roughness profile parameters R_z and R_a as soon as no clear striation marks are recognizable on the surface, or these can be assigned to the roughness profile.

With the help of these tables, it is possible for the operators of a AWJ system to immediately check that the manufactured surface meets the required quality level by means of a simple measuring device such as a mess slider. Since the roughness characteristics R_z and R_a are frequently required parameters in production drawings, it is possible to assign them to a quality level and a range of striation mark displacement and thus to carry out a first quick check on the set cutting parameters. It is also apparent that the areas used for the categorization of roughness ratios overlap greatly. Therefore, it must be reiterated that the *Q* level cannot be clearly determined by measuring roughness characteristics alone. Figure 18 again shows the course of the *RSm* value along with different *Q* for all materials.

Declarations

References

1. Kartal F, Gokkaya H (2013) Turning with abrasive water jet machining—a review. Eng Sci Technol an Int J 16:113–122
2. Naresh Babu M, Muthukrishnan N (2014) Investigation on surface roughness in abrasive water-jet machining by the response surface method. Mater Manuf Process 29. https://doi.org/10.1080/10426914.2014.952020
3. Kumar R, Chattopadhyaya S, Dixit AR et al (2017) Surface integrity analysis of abrasive water jet-cut surfaces of friction stir welded joints. Int J Adv Manuf Technol 88. https://doi.org/10.1007/s00170-016-8776-0
4. den Dunnen S, Mulder L, Kerkhoffs GMMJ et al (2013) Waterjet drilling in porcine bone: the effect of the nozzle diameter and bone architecture on the hole dimensions. J Mech Behav Biomed Mater 27:84–93. https://doi.org/10.1016/j.jmbbm.2013.06.012
5. Perec A, Radomska-Zalas A, Fajdek-Bieda A (2021) Experimental research into marble cutting by abrasive water jet. Facta Univ Ser Mech Eng
6. Manjaiah M, Narendranath S, Basavarajappa S (2014) Review on non-conventional machining of shape memory alloys. Trans Nonferrous Met Soc China 24(1)12–21. https://doi.org/10.1016/S1003-6326(14)63022-3
7. Hreha P, Hloch S, Magurová D et al (2010) Water jet technology used in medicine. Teh Vjesn 17(2):237–40
8. Foldyna J, Sitek L, Martinec P et al (2005) Rock cutting by pulsing water jets. In: Impact of human activity on the geological environment - Proceedings of the International Symposium of the International Society for Rock Mechanics, Eurock 2005
9. Perec A, Radomska-Zalas A (2019) Modeling of abrasive water suspension jet cutting process using response surface method. In: AIP Conference Proceedings. AIP Publishing LLC, p 20051
10. Teti M, Papini M, Spelt JK (2018) Jet properties and mixing chamber flow in a high-pressure abrasive slurry jet: part I—measurement of jet and chamber conditions. Int J Adv Manuf Technol 99:1283–1291. https://doi.org/10.1007/s00170-018-2546-0
11. Folkes J (2009) Waterjet—an innovative tool for manufacturing. J Mater Process Technol 209:6181–6189. https://doi.org/10.1016/j.jmatprotec.2009.05.025
12. Yuvaraj N, Pradeep Kumar M (2014) Multiresponse optimization of abrasive water jet cutting process parameters using TOPSIS approach. Mater Manuf Process 30. https://doi.org/10.1080/10426914.2014.994763
13. Valicek J, Hloch S (2009) Optical measurement of surface and topographical parameters investigation created by abrasive waterjet. Int J Surf Sci Eng 3. https://doi.org/10.1504/IJSURFSE.2009.027421
14. Hreha P, Radvanska A, Carach J et al (2014) Monitoring of focusing tube wear during Abrasive WaterJet (AWJ) cutting of AISI 309. Metalurgija 53:533–536

15. Valíček J, Hloch S, Kozak D (2009) Surface geometric parameters proposal for the advanced control of abrasive waterjet technology. Int J Adv Manuf Technol 41. https://doi.org/10.1007/s00170-008-1489-2

16. Hreha P, Radvanska A, Knapcikova L et al (2015) Roughness parameters calculation by means of on-line vibration monitoring emerging from AWJ interaction with material. Metrol Meas Syst 22:315–326. https://doi.org/10.1515/mms-2015-0024

17. Singh JP, Chen WL, Munoz J (1991) Comprehensive evaluation of abrasive waterjet cut surface quality. In: 6th American Water Jet Conference – Proceedings of the 6th American Water Jet Conference, Houston, TX, WTJA, pp 139–161.

18. Valíček J, Držík M, Hloch S et al (2007) Experimental analysis of irregularities of metallic surfaces generated by abrasive waterjet. Int J Mach Tools Manuf 47. https://doi.org/10.1016/j.ijmachtools.2007.01.004

19. Hashish M (1984) A modeling study of metal cutting with abrasive waterjets. J Eng Mater Technol 106:88–100. https://doi.org/10.1115/1.3225682

20. Kulekci MK (2002) Processes and apparatus developments in industrial waterjet applications. Int J Mach Tools Manuf 42:1297–1306. https://doi.org/10.1016/S0890-6955(02)00069-X

21. Hlaváč LM (2009) Investigation of the abrasive water jet trajectory curvature inside the kerf. J Mater Process Technol 209:4154–4161

22. Hreha P, Radvanská A, Hloch S et al (2015) Determination of vibration frequency depending on abrasive mass flow rate during abrasive water jet cutting. Int J Adv Manuf Technol 77:763–774. https://doi.org/10.1007/s00170-014-6497-9

23. Lemma E, Chen L, Siores E, Wang J (2002) Optimising the AWJ cutting process of ductile materials using nozzle oscillation technique. Int J Mach Tools Manuf 42:781–789. https://doi.org/10.1016/S0890-6955(02)00017-2

24. Perec A (2018) Experimental research into alternative abrasive material for the abrasive water-jet cutting of titanium. Int J Adv Manuf Technol 97:1529–1540

25. Nag A, Ščučka J, Hlavacek P et al (2018) Hybrid aluminium matrix composite AWJ turning using olivine and Barton garnet. Int J Adv Manuf Technol 94:2293–2300. https://doi.org/10.1007/s00170-017-1036-0

26. Perec A, Pude F, Kaufeld M, Wegener K (2017) Obtaining the selected surface roughness by means of mathematical model based parameter optimization in abrasive waterjet cutting. Strojniški vestnik-Journal Mech Eng 63:606–613

27. Chao J, Geskin E (1993) Experimental study of the striation formation and spectral analysis of the abrasive waterjet generated surfaces. 7th American Water Jet Conference. Seattle, Washington, pp 27–41

28. Zeng J, Kim T (1993) Parameter prediction and cost analysis in abrasive waterjet cutting operations. In: Proceedings of the 7th American Water Jet Conference, pp 28–31

29. Miles P, Henning A (2013) Rz: a better measurement of abrasive waterjet cut surface finishes. In: WJTA-IMCA Conference Proceedings

30. Hloch S, Valíček J (2012) Topographical anomaly on surfaces created by abrasive waterjet. Int J Adv Manuf Technol 59:593–604. https://doi.org/10.1007/s00170-011-3511-3

31. Zeng J (2007) Determination of machinability and abrasive cutting properties in AWJ cutting. In: 2007 American Waterjet WJTA Conference. Houston, Texas

32. Perec A (2021) Research into the disintegration of abrasive materials in the abrasive water jet machining process. Materials (Basel) 14:3940

33. Nag A, Hloch S, Dixit AR, Pude F (2020) Utilization of ultrasonically forced pulsating water jet decaying for bone cement removal. Int J Adv Manuf Technol. https://doi.org/10.1007/s00170-020-05892-9

34. Kolb M (2006) Waterjet cutting: material processing with a high-pressure waterjet. Moderne industrie

35. ISO 6508-1: Metallic Materials—Rockwell Hardness Test—Part 1: Test Method. International Organization for Standardization, Geneva (2016).

36. ISO 6506-1-2014: Metallic Materials—Brinell Hardness Test—Part 1: Test Method. International Organization for Standardization, Geneva (2014).

37. BS EN ISO 18265: Metallic Materials. Conversion of Hardness Values. British Standards Institution, London (2013).

38. DIN EN ISO 4287: Geometrical Product Specifications (GPS)—Surface Texture: Profile Method—Terms, Definitions and Surface Texture Parameters; British Standards Institution: London, UK (2010).

39. DIN EN ISO 4288: Geometrical Product Specifications (GPS)-Surface texture: Profile method-Rules and procedures for the assessment of surface texture, Beuth Verlag GmbH, Berlin, Germany (1998).

40. SN 214001. (Contact-free cutting – Water jet cutting – Geometrical product specification and quality). Schweizerische Normen-Vereinigung. 16 s (2010)